


# Farthest-Point Voronoi Diagrams in the Hilbert Metric

Minju Song ✉ 

Graduate School of Artificial Intelligence, Pohang University of Science and Technology,  
Republic of Korea

Mook Kwon Jung ✉

Department of Computer Science and Engineering, Pohang University of Science and Technology,  
Republic of Korea

Hee-Kap Ahn ✉ 

Graduate School of Artificial Intelligence, Department of Computer Science and Engineering,  
Pohang University of Science and Technology, Republic of Korea

---

## Abstract

The Hilbert metric, introduced by David Hilbert in 1895, is a projective metric defined on a bounded convex domain in a Euclidean space. For a convex polygon with  $m$  vertices and  $n$  point sites lying inside the polygon in the plane, it is shown that the nearest-point Voronoi diagram in the Hilbert metric has combinatorial complexity of  $O(mn)$  [Gezalyan and Mount, SoCG 2023]. In this paper, we show that the farthest-point Voronoi diagram in the Hilbert metric has combinatorial complexity  $O(m)$ , which is independent of the number of sites. Also, we present an efficient algorithm to compute the farthest-point Voronoi diagram.

**2012 ACM Subject Classification** Theory of computation → Computational geometry

**Keywords and phrases** Farthest-point Voronoi diagram, Hilbert metric, Complexity, Algorithm

**Digital Object Identifier** 10.4230/LIPIcs.WADS.2025.48

**Funding** This research was supported by the Institute of Information & communications Technology Planning & Evaluation (IITP) grant funded by the Korea government (MSIT) (No. RS-2019-II191906, Artificial Intelligence Graduate School Program (POSTECH)). This research was partly supported by the National Research Foundation of Korea (NRF) grant funded by the Korea government (MSIT) (RS-2023-00219980).

**Acknowledgements** For helpful comments we thank Auguste H. Gezalyan, David M. Mount and the anonymous reviewers.

## 1 Introduction

The Hilbert metric, introduced by David Hilbert in 1895 [16], defines a distance function between points in the interior of any convex body in  $d$ -dimensional space. Hilbert geometry provides a generalized framework that applies to any convex body, transcending the limitations of Euclidean space [21]. The significance of Hilbert metric is highlighted by a critical role in convex approximation, which is widely used in applications such as approximate nearest neighbor searches in the Euclidean metric and other metric spaces [1, 8], optimal construction of  $\epsilon$ -kernels [6], approximate closest vectors [12, 13, 19, 23], and approximations of polytopes with low combinatorial complexity [3, 5, 7]. Various elements used in these approximations, such as Macbeath regions and Dikin ellipsoids, act similarly to Hilbert balls [2].

Despite its potential, not much is known about construction algorithms for structures in Hilbert geometry. Nielsen and Shao characterized balls in the Hilbert metric [20]. Bumpus et al. investigated the properties of balls and bisectors in the Hilbert metric [9]. A Voronoi diagram is one of the most fundamental structures in understanding the underlying geometry.



© Minju Song, Mook Kwon Jung, and Hee-Kap Ahn;  
licensed under Creative Commons License CC-BY 4.0

19th International Symposium on Algorithms and Data Structures (WADS 2025).

Editors: Pat Morin and Eunjin Oh; Article No. 48; pp. 48:1–48:15

Leibniz International Proceedings in Informatics



LIPICs Schloss Dagstuhl – Leibniz-Zentrum für Informatik, Dagstuhl Publishing, Germany

Thus, it has been studied under different metrics [10, 17, 18, 22]. Gezalayan and Mount presented an  $O(mn \log n)$ -time algorithm for computing the nearest-point Voronoi diagram of  $n$  point sites in the Hilbert metric defined by a convex  $m$ -gon [15] and an  $O(n(\log n + \log^3 m))$ -time algorithm for computing the Delaunay triangulation [14]. They showed that the diagram has complexity  $\Theta(mn)$ . No previous work, however, is known about the farthest-point Voronoi diagram in the Hilbert metric. The farthest-point Voronoi diagram may reveal further characteristics of Hilbert geometry and its potential applications.

## 1.1 Our results and outline

We denote by  $\text{FV}(S)$  the farthest-point Voronoi diagram of  $n$  point sites in the Hilbert metric defined by a convex  $m$ -gon  $\Omega$ . Unlike Voronoi diagrams in the Euclidean metric,  $\text{FV}(S)$  poses a few difficulties in the computation. The Hilbert distance between points is defined as the logarithm of the cross-ratio of them and the intersections of the line through the points with the domain boundary. It takes  $O(\log m)$  time to compute the distance between points. The bisector between any two sites is a piecewise conic curve consisting of  $O(m)$  segments. Thus, a naïve divide-and-conquer algorithm using bisectors may take  $\Omega(\min\{nm, m^2\})$  time.

We show that  $\text{FV}(S)$  has combinatorial complexity  $\Theta(m)$ , which is independent of the number of sites. Moreover, we present an  $O(n(\log n + \log^2 m) + m \log n)$ -time algorithm for computing the diagram. This is the first algorithm for computing  $\text{FV}(S)$ .

In Section 2, we introduce the Hilbert metric, Hilbert balls, Hilbert bisectors, and  $\text{FV}(S)$ . In the Euclidean metric, a site of  $S$  has a nonempty cell in the farthest-point Voronoi diagram if and only if it is a vertex of the convex hull of  $S$  [11]. This is, however, not always the case in the Hilbert metric. If a site has a nonempty cell in  $\text{FV}(S)$ , it is a vertex of the convex hull. But not every vertex of the convex hull always has a nonempty cell in  $\text{FV}(S)$ . In Section 3, we characterize this phenomenon and show that each cell in  $\text{FV}(S)$  is connected and incident to the boundary of  $\Omega$ . We give an ordering lemma for the sites of  $S$  and their Voronoi cells appearing along the boundary of  $\Omega$ .

In Section 4, we analyze the combinatorial complexity of  $\text{FV}(S)$ . We show that  $\text{FV}(S)$  has  $O(m)$  edges and each Voronoi cell is connected. Using this, we show that the number of sites with nonempty cells is  $O(m)$ . By Euler's formula, we show that  $\text{FV}(S)$  has  $O(m)$  vertices. We conclude that the combinatorial complexity of  $\text{FV}(S)$  is  $O(m)$ . Additionally, since the complexity of  $\text{FV}(S)$  is at least the complexity of  $\Omega$ , a lower bound on the combinatorial complexity of  $\text{FV}(S)$  is  $\Omega(m)$ . As a result, we give a tight upper bound on the combinatorial complexity of  $\text{FV}(S)$ , which is  $\Theta(m)$  and independent of the number of the sites of  $S$ .

In Section 5, we give an efficient algorithm of  $O(n(\log n + \log^2 m) + m \log n)$  time for computing  $\text{FV}(S)$ . Our algorithm consists of three stages. The subsections in Section 5 describe these stages of the algorithm. In the first stage, we compute the convex hull of  $S$  and remove the points contained in the interior of the convex hull of  $S$ . In the second stage, we construct  $\text{FV}(S)$  restricted to the boundary of  $\Omega$  incrementally by adding the sites of  $S$  one by one in clockwise orientation along the convex hull of  $S$ . In doing so, we maintain a list  $\mathcal{L}$  of sites that have nonempty boundary cell. Initially,  $\mathcal{L}$  contains the first two consecutive sites of  $S$ . When the next site  $s$  is added, we check whether  $s$  is the farthest from an intersection point of the boundary cells corresponding to the first and the last sites stored in  $\mathcal{L}$ . If  $s$  is not the farthest one from the point, it has an empty cell so we are done and move on to the next iteration. If  $s$  is the farthest one, it has a nonempty cell so we append  $s$  to  $\mathcal{L}$ . We compute the boundary cell of  $s$  along the boundary of  $\Omega$  from the intersection point. In this way, we compute all sites of  $S$  whose Voronoi cell is nonempty in  $O(n(\log n + \log^2 m))$  time.

In the third stage, we construct  $\text{FV}(S)$  by subdividing  $\Omega$  into Voronoi cells using  $\text{FV}(S)$  restricted to the boundary of  $\Omega$ . Our algorithm uses a divide-and-conquer technique similar to the one by Shamos and Hoey [24] that computes the nearest-site Voronoi diagram in the plane under the Euclidean metric. Roughly speaking, we partition a site sequence into two subsequences,  $S_L$  and  $S_R$ , of roughly equal size, and compute  $\text{FV}(S_L \cup S_R)$  by merging  $\text{FV}(S_L)$  and  $\text{FV}(S_R)$  along their bisector recursively. But the merge step requires a novel algorithmic idea and an in-depth analysis as each bisector is a piecewise conic curve consisting of  $O(m)$  segments. In each recursive step, we compute approximate bisectors such that they become the exact bisectors in the last recursive depth. We show that this can be done in  $O(m \log \min\{m, n\})$  time in total. Therefore,  $\text{FV}(S)$  can be computed in  $O(n(\log n + \log^2 m) + m \log n)$  time in total.

## 2 Preliminaries

For any two points  $p, q \in \mathbb{R}^d$ , we denote the line segment connecting  $p$  and  $q$  by  $pq$ , and denote the Euclidean distance between  $p$  and  $q$  by  $|pq|$ . A set  $X$  of points is *convex* if for any two points  $p, q \in X$ , every point  $t \in pq$  is contained in  $X$ . The *convex hull* of  $X$  is the smallest convex set that contains  $X$ , which we denote by  $\text{conv}(X)$ . We denote the boundary of  $X$  by  $\partial X$  and the interior of  $X$  by  $\text{int}(X)$ . For any two points  $p, q \in \Omega$ , let  $\chi(p, q)$  denote the intersection of the line through two points  $p$  and  $q$  with  $\Omega$ .

### 2.1 The Hilbert metric and Hilbert balls

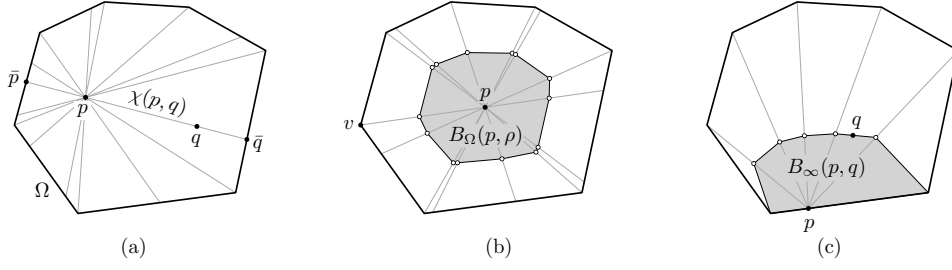
► **Definition 1** (Hilbert metric). *Given a convex body  $\Omega$  and two points  $p, q \in \text{int}(\Omega)$ , let  $\bar{p}$  and  $\bar{q}$  denote the endpoints of  $\chi(p, q)$  such that  $\bar{p}, p, q, \bar{q}$  appear in order along  $\chi(p, q)$ . See Figure 1(a). The Hilbert distance  $d(p, q)$  between  $p$  and  $q$  is defined as*

$$d(p, q) = \frac{1}{2} \ln \left( \frac{|\bar{q}p| |\bar{p}q|}{|\bar{q}q| |\bar{p}p|} \right).$$

The quantity in the logarithm is the cross-ratio of  $(p, q; \bar{q}, \bar{p})$ . If  $p$  or  $q$  lies on  $\partial\Omega$ ,  $d(p, q)$  can be formally defined to be  $+\infty$ . This corresponds to a limiting case that a denominator approaches zero. The Hilbert distance  $d$  is extended to all pairs of points by letting  $d(p, p) = 0$ . It satisfies the axioms of a metric, and in particular, it is symmetric and the triangle inequality holds. Observe  $d(p, q) + d(q, r) = d(p, r)$  if  $p, q$ , and  $r$  are collinear in  $\Omega$  [21].

In the remainder of the paper, we abuse the notation and use  $\Omega$  to denote a convex polygon with  $m$  vertices in the plane. For any two points  $p, q \in \text{int}(\Omega)$ , a simple binary search makes it possible to determine the two edges of  $\partial\Omega$ , each containing an endpoint of  $\chi(p, q)$ . Thus, the Hilbert distance between two points can be computed in  $O(\log m)$  time.

For a point  $p \in \text{int}(\Omega)$  and  $\rho > 0$ , let  $B_\Omega(p, \rho)$  denote the *Hilbert ball* of radius  $\rho$  centered at  $p$ . Nielsen and Shao characterized the shape of Hilbert balls and showed how to compute them [20]. Consider the set of  $\chi(p, v)$ 's for vertices  $v$  of  $\Omega$ , which we call the *spokes* of  $p$ . See Figure 1(a). For each  $\chi(p, v)$ , there are exactly two points lying on  $\chi(p, v)$  whose Hilbert distance from  $p$  is  $\rho$ . Those points are all in convex position. Then  $B_\Omega(p, \rho)$  is the convex polygon with vertices on those  $2m$  points. We say  $B_\Omega(p, \rho)$  is the Hilbert ball centered at  $p$  with radius  $\rho$ . For a point  $x \in B_\Omega(p, \rho)$ ,  $d(p, x) \leq \rho$ ; the equality holds for  $x$  lying on the boundary of  $B_\Omega(p, \rho)$ . For a point  $x \in \Omega \setminus B_\Omega(p, \rho)$ ,  $d(p, x) > \rho$ . See Figure 1(b).

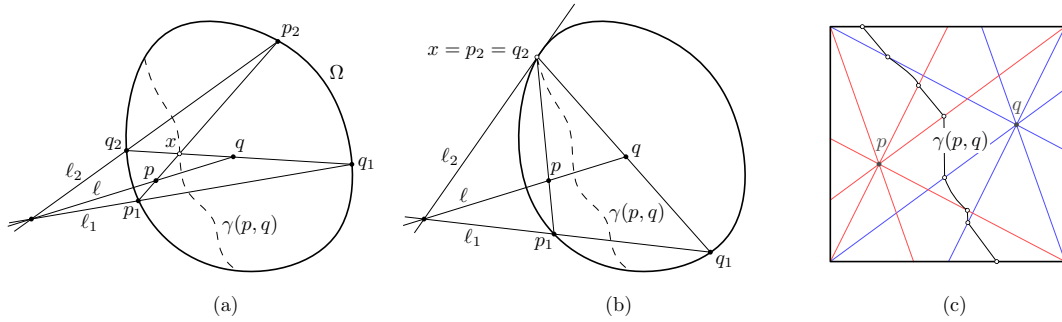


■ **Figure 1** (a) The endpoints  $\bar{p}$  and  $\bar{q}$  of  $\chi(p, q)$  and spokes defined by  $p$ . (b) For any point  $x$  in the boundary of  $B_\Omega(p, \rho)$ ,  $d(p, x) = \rho$ . (c) The infinite Hilbert ball  $B_\infty(p, q)$ .

We extend the concept of Hilbert balls to ones centered at points in  $\partial\Omega$ , which we call *infinite Hilbert balls*. Let  $p$  be a point in  $\partial\Omega$ , and let  $q$  be a point in  $\text{int}(\Omega)$ . For arbitrarily small  $\delta > 0$ , let  $p_\delta$  be the point on  $pq$  with  $|pp_\delta| = \delta$ . As  $\delta$  approaches 0, any sequence of Hilbert balls in the family  $\{B_\Omega(p_\delta, d(p_\delta, q))\}$  converges to the infinite Hilbert ball centered at  $p$  with radius  $d(p_\delta, q) = d(p, q)$ , which we denote by  $B_\infty(p, q)$ . See Figure 1(c).

## 2.2 Hilbert bisectors

Gezalyan and Mount [15] introduced the *Hilbert bisector* of two points  $p, q \in \text{int}(\Omega)$ , denoted by  $\gamma(p, q)$ , which is the set of points  $x \in \Omega$  satisfying  $d(x, p) = d(x, q)$ . For any point  $x \in \gamma(p, q) \cap \text{int}(\Omega)$ ,  $q \in \partial B_\Omega(x, d(x, p))$  and  $p \in \partial B_\Omega(x, d(x, q))$ . For any point  $x \in \gamma(p, q) \cap \partial\Omega$ ,  $q \in \partial B_\infty(x, p)$  and  $p \in \partial B_\infty(x, q)$ . For a point  $x \in \Omega$ , let  $p_1, p_2$  be two endpoints of  $\chi(x, p)$ , and let  $q_1, q_2$  be two endpoints of  $\chi(x, q)$ . Let  $\ell_1, \ell$ , and  $\ell_2$  be the lines containing the segments  $p_1q_1$ ,  $pq$ , and  $p_2q_2$ , respectively. If  $x \in \partial\Omega$ , let  $x = p_2 = q_2$  and let  $\ell_2$  be the line tangent to  $\Omega$  at  $x$ . It is shown that two cross ratios,  $(x, p; p_1, p_2)$  and  $(x, q; q_1, q_2)$ , are the same if and only if these three lines meet at a common point. It follows  $d(x, p) = d(x, q)$ , and thus  $x$  is on the bisector. See Figure 2(a-b).



■ **Figure 2**  $\gamma(p, q)$  for cases (a)  $x \in \text{int}(\Omega)$  and (b)  $x \in \partial\Omega$ . (c) The subdivision of  $\Omega$  (square) by the spokes of  $p$  (red) and  $q$  (blue).  $\gamma(p, q)$  is a piecewise conic curve with joints on the spokes of  $p$  and  $q$ .

The Hilbert distances  $d(p, x)$  and  $d(q, x)$  of a point  $x \in \text{int}(\Omega)$  are determined by the boundary edges of  $\Omega$  incident to  $\chi(p, x)$  and  $\chi(q, x)$ , respectively. Consider the subdivision of  $\Omega$  by all spokes of  $p$  and all spokes of  $q$ . Observe that for every point  $x$  in a subregion, the set of edges of  $\partial\Omega$  incident to  $\chi(p, x)$  and  $\chi(q, x)$  remains the same. Thus,  $d(p, x)$  and  $d(q, x)$  for points  $x$  in a subregion can be formulated in explicit functions, and thus we can obtain the Hilbert bisector of  $p$  and  $q$  restricted to the subregion from the functions. It has

been shown that  $\gamma(p, q)$  in a subregion is a conic curve. It follows that  $\gamma(p, q)$  is a piecewise conic curve whose joints lie on subregion boundaries [9]. Thus, we say that  $\gamma(p, q)$  consists of *bisector segments*. See Figure 2(c).

► **Lemma 2** (Lemma 2 of [14]). *For any three points in  $\text{int}(\Omega)$  not lying on the same line, there is at most one Hilbert ball whose boundary contains them.*

Lemma 2 naturally extends for infinite Hilbert balls. The lemma implies that  $\gamma(p, q) \cap \gamma(q, r)$  is at most one point for any three points  $p, q, r \in \text{int}(\Omega)$  not lying on the same line.

► **Lemma 3.** *Two distinct (infinite) Hilbert balls intersect each other along their boundaries in at most two connected components.*

### 2.3 Farthest-point Voronoi diagram

Let  $S$  be a set of  $n$  points lying in  $\text{int}(\Omega)$  which we call *sites*. The *farthest-point Voronoi diagram* of  $S$  in the Hilbert distance on  $\Omega$ , denoted by  $\text{FV}(S)$ , is a subdivision of  $\Omega$  into cells in which the same point of  $S$  is the farthest point in the Hilbert distance. The *farthest-point Voronoi cell* of a site  $s \in S$ , denoted by  $V(s)$ , is the set of points whose farthest site is  $s$  in the Hilbert distance. Consider a point  $p \in \Omega$  contained in  $V(s)$ . If  $p \in \text{int}(\Omega)$ ,  $d(p, s) \geq d(p, s')$  for all sites  $s' \in S$ . If  $p \in \partial\Omega$ , there is a point sequence  $\{q_i\}_{i \in \mathbb{N}}$  contained in  $\text{int}(\Omega)$  such that the sequence converges to  $p$  and  $d(q_i, s) \geq d(q_i, s')$  for all sites  $s' \in S$  and for all  $i \in \mathbb{N}$ . Not every point of  $S$  has a nonempty cell in  $\text{FV}(S)$ . We will investigate this in Section 3.

**General Position Assumption.** We assume that no three sites in  $S$  are collinear, and in particular, the line passing through any pair of sites of  $S$  and the lines extending any two edges of  $\Omega$  are not coincident at a common point, including all three being parallel. If this assumption does not hold, the bisectors separating Voronoi cells can widen into 2-dimensional regions. These general position conditions were also assumed by Gezalyn and Mount [15].

## 3 Conditions for valid sites

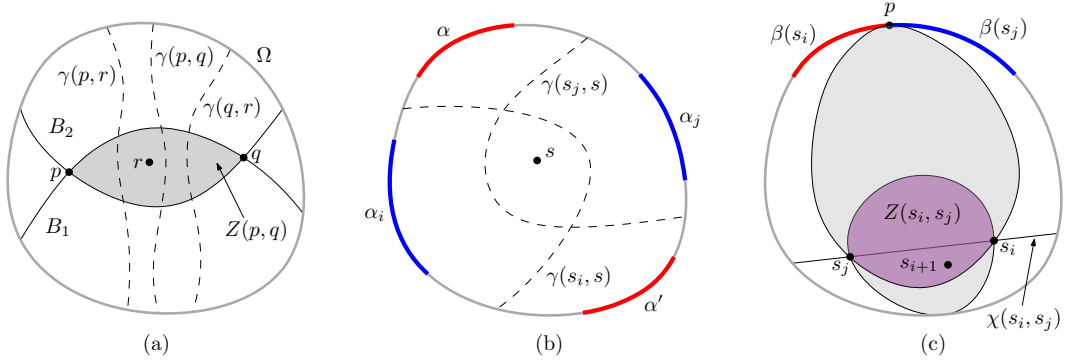
We study the conditions for a site to have a nonempty cell in  $\text{FV}(S)$ . We say a site  $s \in S$  is *valid* for  $\text{FV}(S)$  if  $V(s) \neq \emptyset$ . As for the farthest-point Voronoi diagram in the Euclidean metric, a site contained in the interior of  $\text{conv}(S)$  cannot have a nonempty cell in  $\text{FV}(S)$ .

► **Lemma 4.** *If a site  $s$  is contained in  $\text{int}(\text{conv}(S))$ ,  $s$  is not valid for  $\text{FV}(S)$ .*

**Proof.** Suppose that  $s \in \text{int}(\text{conv}(S))$  is valid for  $\text{FV}(S)$ . Then there is a point  $p \in V(s)$  such that  $d(p, s) \geq d(p, s')$  for all  $s' \in S$ . This implies that  $B_\Omega(p, d(p, s))$  contains all sites of  $S$ . Since  $B_\Omega(p, d(p, s))$  is convex,  $\text{conv}(S)$  is contained in  $B_\Omega(p, d(p, s))$ . Then  $s \in \text{int}(\text{conv}(S)) \subseteq \text{int}(B_\Omega(p, d(p, s)))$ , contradicting that  $s$  lies on the boundary of  $B_\Omega(p, d(p, s))$ . ◀

In the Euclidean metric, every site has a nonempty cell in the farthest-point Voronoi diagram if it appears as a vertex of the convex hull of the sites. This is not necessarily true for  $\text{FV}(S)$  in the Hilbert metric. For two distinct points  $p, q \in \text{int}(\Omega)$ , let  $B_1$  and  $B_2$  be two infinite Hilbert balls, each of which contains both  $p$  and  $q$  on its boundary. Let  $Z(p, q) = B_1 \cap B_2$ . Gezalyn et al. [14] showed that no Hilbert ball contains  $p, q$ , and a point  $r \in \text{int}(Z(p, q))$  on its boundary. Using Lemma 2, they showed that every Hilbert ball centered at a point in  $\gamma(p, q)$  and containing both  $p$  and  $q$  on its boundary contains  $Z(p, q)$ . See Figure 3(a).

► **Lemma 5.** *If a site is contained in  $Z(p, q)$  for sites  $p$  and  $q$ , it is not valid for  $\text{FV}(S)$ .*



■ **Figure 3** (a)  $Z(p, q) = B_1 \cap B_2$  for two infinite Hilbert balls  $B_1$  and  $B_2$  with  $p \in \partial B_1$  and  $q \in \partial B_2$ .  $\gamma(p, q)$  separates  $\gamma(p, r)$  from  $\gamma(q, r)$ . (b)  $\alpha_i, \alpha, \alpha_j, \alpha'$  appear in clockwise orientation along  $\partial \Omega$ . (c) Two infinite Hilbert balls, each containing both  $s_i$  and  $s_j$  on its boundary. Then  $s_{i+1} \in Z(s_i, s_j)$ .

**Proof.** Let  $r$  be a site contained in  $Z(p, q)$  for some sites  $p$  and  $q$ . Then no Hilbert ball contains  $p$ ,  $q$ , and  $r$  on its boundary [14]. This implies that  $\gamma(p, r)$  does not intersect  $\gamma(q, r)$ . Without loss of generality, we assume that  $\gamma(p, q)$  separates  $p$  and  $r$  from  $q$ . Let  $x$  be a point contained in  $\gamma(p, q)$ . Since the Hilbert ball centered at  $x$  and containing  $p$  and  $q$  on its boundary contains  $r$ ,  $d(x, r) < d(x, p) = d(x, q)$ . This means that  $\gamma(p, r)$  separates  $r$  and  $x$  from  $p$ , and  $\gamma(q, r)$  separates  $r$  and  $x$  from  $q$ . Since  $\gamma(p, q)$  does not intersect  $\gamma(p, r)$  and  $\gamma(q, r)$ ,  $\gamma(p, q)$  separates  $\gamma(p, r)$  from  $\gamma(q, r)$ . Then the side of  $\gamma(p, r)$  containing  $p$  does not intersect the side of  $\gamma(q, r)$  containing  $q$ . Since  $V(r) = \{x \in \Omega \mid \cap_{s \in S} d(x, s) \leq d(x, r)\}$ , we have  $V(r) = \emptyset$ , and thus  $r$  is not valid for  $\text{FV}(S)$ . See Figure 3(a) for an illustration. ◀

By Lemma 5, a site  $r \in S$  may be not valid for  $\text{FV}(S)$  even for  $r \notin \text{int}(\text{conv}(S))$ .

### 3.1 $\text{FV}(S)$ restricted to the domain boundary

To find all valid sites of  $S$  for  $\text{FV}(S)$  and compute  $\text{FV}(S)$  efficiently, we compute  $\text{FV}(S)$  restricted to the boundary of  $\Omega$ . We denote it by  $\text{bFV}(S)$ . The Voronoi cell in  $\text{bFV}(S)$  of a site  $s \in S$ , denoted by  $\beta(s)$ , is the intersection of  $V(s)$  and  $\partial \Omega$ . We call a site  $s \in S$  *valid* for  $\text{bFV}(S)$  if  $\beta(s) \neq \emptyset$ .

► **Lemma 6.** Let  $p$  be a point in  $V(s)$  and  $\bar{p}$  be the endpoint of  $\chi(s, p)$  closer to  $p$  than to  $s$ . Then  $p\bar{p} \subseteq V(s)$ .

**Proof.** Suppose there is a point  $r \in p\bar{p}$  but  $r \notin V(s)$ . Let  $t$  be a site of  $S$  with  $r \in V(t)$ . By definition,  $d(s, p) \geq d(t, p)$  and  $d(t, r) > d(s, r)$ . Combining these we have  $d(s, p) + d(t, r) > d(t, p) + d(s, r)$ , or equivalently  $d(t, r) > d(t, p) + d(s, r) - d(s, p) = d(t, p) + d(p, r)$  as  $s, p, r$  are collinear [21]. But this violates the triangle inequality, yielding a contradiction. ◀

Since  $\text{bFV}(S)$  is the restriction of  $\text{FV}(S)$  on the boundary of  $\Omega$ , a site valid for  $\text{bFV}(S)$  is also valid for  $\text{FV}(S)$ . Lemma 6 implies that a site valid for  $\text{FV}(S)$  is also valid for  $\text{bFV}(S)$ . Thus, we can identify all valid sites of  $S$  for  $\text{FV}(S)$  from  $\text{bFV}(S)$ .

► **Lemma 7.**  $\beta(s)$  is connected for a site  $s \in S$ .

**Proof.** If  $s$  is not valid for  $\text{FV}(S)$ ,  $\beta(s) = \emptyset$  and we are done. Assume for the contradiction that  $s$  is valid for  $\text{FV}(S)$  and  $\beta(s)$  is not connected for a site  $s \in S$ . Let  $\alpha$  and  $\alpha'$  be two connected components of  $\beta(s)$ . Then there are two sites  $s_i, s_j \in S \setminus \{s\}$ , not necessarily

distinct, with connected components  $\alpha_i$  of  $\beta(s_i)$  and  $\alpha_j$  of  $\beta(s_j)$  such that  $\alpha_i, \alpha, \alpha_j, \alpha'$  appear in order along  $\partial\Omega$  in clockwise orientation, as shown in Figure 3(b). Observe that  $\alpha_i$  and  $\alpha$  are separated by  $\gamma(s_i, s)$ , and  $\alpha_j$  and  $\alpha'$  are separated by  $\gamma(s_j, s)$ . Since both the side of  $\gamma(s_i, s)$  containing  $\alpha_i$  and the side of  $\gamma(s_j, s)$  containing  $\alpha_j$  contain  $s$ ,  $\gamma(s_i, s)$  and  $\gamma(s_j, s)$  intersect at least two times. Since  $s, s_i$ , and  $s_j$  are not collinear, this contradicts Lemma 2. ◀

By Lemmas 6 and 7,  $\beta(s)$  is nonempty and connected for every valid site  $s$  of  $S$ . Aronov et al. [4] gave an *Ordering Lemma* for the farthest-point geodesic Voronoi diagram for point sites in a simple polygon. We extend the ordering lemma for  $\text{FV}(S)$  with respect to  $\partial\Omega$ .

► **Lemma 8.** *The order of valid sites along their convex hull is the same as the order of their Voronoi cells along the boundary of  $\Omega$ .*

**Proof.** For ease of description, we relabel the sites such that  $\langle s_0, s_1, \dots, s_{t-1} \rangle$  is the sequence of sites valid for  $\text{FV}(S)$  in clockwise orientation along their convex hull. We use modulo  $t$  for indices. First, we show that  $\beta(s_i)$  and  $\beta(s_{i+1})$  are adjacent to each other for every  $i = 0, \dots, t-1$ . Suppose that  $\beta(s_i)$  and  $\beta(s_{i+1})$  are not adjacent to each other for some  $i$ . Let  $s_j$  be a site such that  $\beta(s_j)$  and  $\beta(s_i)$  are adjacent to each other and  $\beta(s_j)$  appears right after  $\beta(s_i)$  in clockwise orientation along  $\partial\Omega$ . Since  $p = \beta(s_i) \cap \beta(s_j)$  is an endpoint of  $\gamma(s_i, s_j)$ ,  $B_\infty(p, s_i)$  and  $B_\infty(p, s_j)$  are the same. Then  $s_{i+1}, s_{j+1} \in B_\infty(p, s_i)$ . See Figure 3(c).

Observe that  $\chi(s_i, s_j)$  separates  $s_{i+1}$  from  $s_{j+1}$  since all sites  $\langle s_0, s_1, \dots, s_{t-1} \rangle$  appear in clockwise orientation along their convex hull. Without loss of generality, assume that  $s_{i+1}$  is contained in the side of  $\chi(s_i, s_j)$  not containing  $p$ . Let  $q$  be the endpoint of  $\gamma(s_i, s_j)$  other than  $p$ . Thus,  $q$  is contained in the side of  $\chi(s_i, s_j)$  containing  $s_{i+1}$ . Then  $B_\infty(q, s_i)$  and  $B_\infty(q, s_j)$  are the same, and thus  $B_\infty(q, s_i)$  contains both  $s_i$  and  $s_j$  on its boundary. By Lemma 3,  $B_\infty(p, s_i)$  and  $B_\infty(q, s_i)$  intersect each other along their boundaries at most twice. Thus,  $s_{i+1}$  is contained in  $B_\infty(q, s_i)$ . Since  $s_{i+1} \in B_\infty(p, s_i) \cap B_\infty(q, s_i)$ , it follows from Lemma 5 that  $s_{i+1}$  is not valid for  $\text{FV}(S)$ . This is a contradiction that  $s_{i+1}$  is valid. Thus,  $\beta(s_i)$  and  $\beta(s_{i+1})$  are adjacent to each other.

There are two cases:  $\langle \beta(s_0), \dots, \beta(s_{t-1}) \rangle$  appear in order in clockwise orientation along  $\partial\Omega$  or they appear in order in counterclockwise orientation along  $\partial\Omega$ . Suppose the latter case. Then for some  $i$ , the side of  $\chi(s_{i-1}, s_{i+1})$  containing  $s_i$  contains a point in  $\beta(s_i)$ . Let  $p$  and  $q$  be the endpoints of  $\gamma(s_{i-1}, s_{i+1})$  such that  $\beta(s_{i-1}), p, \beta(s_{i+1})$ , and  $q$  appear in clockwise orientation along  $\partial\Omega$ . By definition,  $s_i$  is contained in  $B_\infty(p, s_{i+1})$ . Observe that  $s_i$  is contained in  $B_\infty(q, s_{i+1})$  by the argument in the previous paragraph. Thus,  $s_i$  is contained in  $Z(s_{i-1}, s_{i+1})$ . By Lemma 5,  $s_i$  is not valid for  $\text{FV}(S)$ , a contradiction. Thus,  $\beta(s_1), \dots, \beta(s_n)$  appear in order in clockwise orientation along  $\partial\Omega$ . ◀

## 4 Complexity

We analyze the combinatorial complexity of  $\text{FV}(S)$  by counting the numbers of vertices, bisector segments, and edges of  $\text{FV}(S)$ . Let  $\hat{S} = \{s_0, s_1, \dots, s_{t-1}\}$  denote the set of sites valid for  $\text{FV}(S)$  such that  $s_0, s_1, \dots, s_{t-1}$  appear in clockwise orientation along their convex hull. We use modulo  $t$  for the indices of the sites in  $\hat{S}$ . Obviously,  $\text{FV}(S)$  and  $\text{FV}(\hat{S})$  are the same.

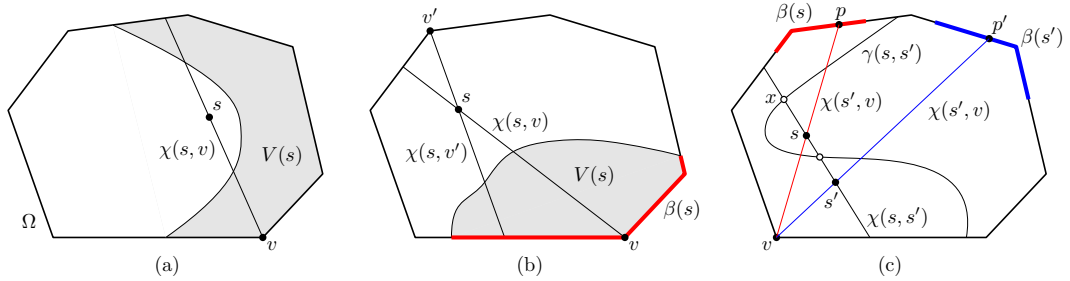
For two sites  $s, s' \in \hat{S}$ , we call each connected portion of  $\gamma(s, s')$  that appears in  $\text{FV}(\hat{S})$  a *Voronoi edge* defined by  $s$  and  $s'$ . Thus, a Voronoi edge is a curve consisting of bisector segments of  $\gamma(s, s')$ , with the exception that the first and last segments might be truncated. Each endpoint of a Voronoi edge is a *Voronoi vertex*, which has degree 3 (if contained in the interior of  $\Omega$ ) or 1 (if contained in  $\partial\Omega$ ). Each endpoint of a bisector segment is either a Voronoi vertex or a vertex with degree 2. We show that  $\text{FV}(\hat{S})$  has  $O(m)$  Voronoi edges,

and that  $\text{FV}(\hat{S})$  consists of  $O(m)$  Voronoi cells and  $O(m)$  Voronoi vertices. This implies that  $\text{FV}(\hat{S})$  has complexity  $O(m)$ . Since the complexity of  $\text{FV}(\hat{S})$  is at least the complexity of  $\Omega$ ,  $\text{FV}(\hat{S})$  has complexity  $\Omega(m)$ . Thus, the combinatorial complexity of  $\text{FV}(\hat{S})$  is  $\Theta(m)$ .

#### 4.1 Complexity of $\text{FV}(S)$

Gezalyan and Mount [15] showed that the combinatorial complexity of the nearest-point Voronoi diagram is  $O(mn)$ . We show that the combinatorial complexity of the farthest-point Voronoi diagram is  $O(m)$ . Recall that every bisector is a piecewise conic with joints lying on spokes. To analyze the combinatorial complexity of  $\text{FV}(S)$ , we count the number of Voronoi vertices and the total number of bisector segments in  $\text{FV}(S)$ . Let  $\kappa(p)$  denote the set of farthest sites for a point  $p$  in  $\partial\Omega$ . If  $\kappa(p)$  consists of a single element, we use  $\kappa(p)$  to denote the element. The following lemma shows an upper bound on the number of bisector segments.

► **Lemma 9.** *There are  $O(m)$  bisector segments in  $\text{FV}(S)$ .*



■ **Figure 4** (a)  $\chi(s_i, v)$  crosses  $\partial V(s_i)$  at most twice. (b)  $\chi(s, v)$  for  $v \in \beta(s)$  and  $\chi(s, v')$  for  $v' \notin \beta(s)$  cross  $\partial V(s)$ . (c) A point  $x \in \chi(s, s') \cap \chi(s', v)$  not contained in  $ss'$ .

**Proof.** We count the number of bisector segments in  $\text{FV}(S)$  by counting the spokes of  $s$  that cross the boundary of  $V(s)$  for each  $s \in S$ . Consider a bisector segment  $\sigma$  of  $\gamma(s_i, s_j)$  in  $\text{FV}(S)$  for two sites  $s_i$  and  $s_j$ . Since  $\gamma(s_i, s_j)$  is a piecewise conic with joints on spokes of  $s_i$  and  $s_j$ , each endpoint of  $\sigma$  lies on a spoke of  $s_i$  or  $s_j$  unless it is a Voronoi vertex. Let  $v$  be a vertex of  $\Omega$  such that an endpoint of  $\sigma$  lies on  $\chi(s_i, v)$ . Then  $\chi(s_i, v)$  intersects  $V(s_i)$ . By Lemma 6,  $\chi(s_i, v)$  intersects at most two bisector segments in  $\partial V(s_i)$ . See Figure 4(a). This implies that the number of bisector segments in  $\text{FV}(S)$  can be obtained by counting the total number of spokes of  $s$  that intersect  $\partial V(s)$  for each  $s \in S$ .

Consider  $\chi(s, v)$  for a site  $s$  and a vertex  $v$  of  $\Omega$  such that  $\chi(s, v) \cap V(s) \neq \emptyset$ . Then either  $v \in \beta(s)$  or  $v \notin \beta(s)$ . See Figure 4(b). If  $v \in \beta(s)$ ,  $v$  is incident to at most two Voronoi cells, and thus the total number of such spokes is  $O(m)$ .

Consider the case that  $v \notin \beta(s)$ . Assume for the contradiction that there is another site  $s' (\neq s)$  such that  $\chi(s', v) \cap V(s') \neq \emptyset$  but  $v \notin \beta(s')$ . Let  $p$  be the intersection of  $\chi(s, v)$  and  $\beta(s)$ , and let  $p'$  be the intersection of  $\chi(s', v)$  and  $\beta(s')$ . See Figure 4(c). If  $v, s$ , and  $s'$  are collinear,  $p = p'$  and  $\kappa(p) = \kappa(p')$ , implying  $s = s'$ .

So assume that  $v, s$ , and  $s'$  are not collinear. Since  $\gamma(s, s')$  separates  $\beta(s)$  and  $s'$  from  $\beta(s')$  and  $s$ ,  $\gamma(s, s')$  crosses each of  $ps$ ,  $ss'$ , and  $s'p'$  in an odd number of times. Thus, there is a point  $x$  on  $\chi(s, s') \cap \gamma(s, s')$  that is not contained in  $ss'$ . By definition,  $d(x, s) = d(x, s')$ . Since  $x, s$ , and  $s'$  are all contained in  $\chi(s, s')$ , we have  $d(x, s') = d(x, s) + d(s, s')$  or  $d(x, s) = d(x, s') + d(s, s')$ , implying that  $d(s, s') = 0$  and thus  $s = s'$ .

Hence, the total number of such spokes is  $O(m)$ . Since there are  $O(m)$  spokes that cross cell boundaries in  $\text{FV}(S)$ , the total number of bisector segments in  $\text{FV}(S)$  is  $O(m)$ . ◀

It remains to count the number of Voronoi vertices, which can be done by Euler's formula.

► **Lemma 10.** *For a site  $s \in S$ ,  $V(s)$  is connected.*

**Proof.** Assume for the contradiction that  $V(s)$  is not connected for a site  $s \in S$ . Let  $C_1$  and  $C_2$  be two connected components of  $V(s)$ . For each  $i = 1, 2$ , let  $p_i$  be a point lying inside  $C_i$ , and let  $q_i$  be the point closer to  $p_i$  than  $s$  among two endpoints of  $\chi(s, p_i)$ . By Lemma 6,  $p_i q_i \subseteq V(s)$ . However,  $q_1$  and  $q_2$  are not connected in  $\beta(s)$ , which contradicts Lemma 7. ◀

► **Lemma 11.** *There are  $O(m)$  sites in  $FV(S)$ .*

**Proof.** By Lemmas 6 and 9, there are  $O(m)$  sites valid for  $\text{bFV}(S)$ . Thus, there are  $O(m)$  sites in  $FV(S)$  by Lemma 8. ◀

► **Theorem 12.** *The farthest-point Voronoi diagram of  $n$  point sites lying inside a convex  $m$ -gon in the Hilbert metric has combinatorial complexity  $O(m)$ .*

**Proof.** By Lemmas 10 and 11, the number of Voronoi cells is  $O(m)$ . Since the number of bisector segments is  $O(m)$  by Lemma 9, the number of Voronoi edges is  $O(m)$ . By Euler's formula, the number of Voronoi vertices is  $O(m)$ . ◀

## 5 Algorithm

In this section, we present an algorithm to compute  $FV(S)$ . Our algorithm computes  $\text{bFV}(S)$  and identifies all valid sites. Then it computes  $FV(S)$  in a divide-and-conquer manner.

### 5.1 Computing $FV(S)$ restricted to the domain boundary

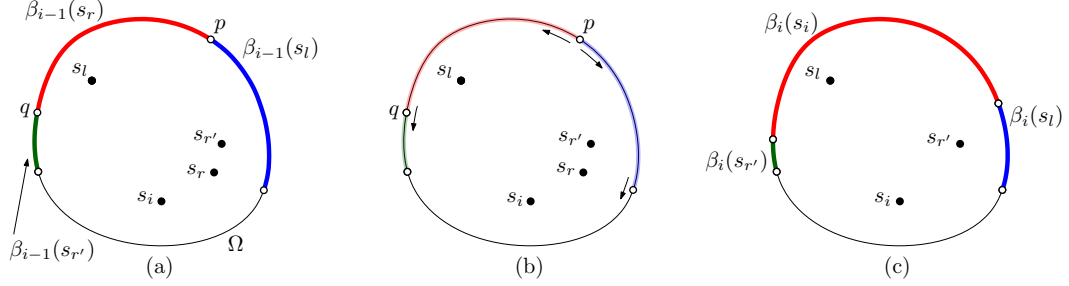
By Lemma 4, every site of  $S$  contained in  $\text{int}(\text{conv}(S))$  is not valid for  $FV(S)$ . Hence, we compute  $\text{conv}(S)$  and remove all sites contained in its interior from  $S$ . This can be done in  $O(n \log n)$  time. Thus, all remaining sites in  $S$  are in convex position. We relabel them such that  $\langle s_1, s_2, \dots, s_n \rangle$  is the sequence of sites in clockwise orientation along their convex hull.

Some sites of  $S$ , however, may not be valid for  $FV(S)$ . We will identify all valid sites of  $S$  by computing  $\text{bFV}(S)$ . We do this incrementally by inserting sites one by one in order, checking if the newly inserted one is valid for the Voronoi diagram of the sites inserted so far, and handling the cases accordingly. We maintain a few structures. Let  $S_i$  be the subset of  $S$  consisting of the first  $i$  sites of  $S$  for  $i = 2, \dots, n$ . Let  $\beta_i(s)$  denote the Voronoi cell of  $s \in S_i$  in  $\text{bFV}(S_i)$ . Let  $\mathcal{L}_i$  be the list that maintains all valid sites for  $FV(S_i)$ .

Initially, let  $S_2 = \{s_1, s_2\}$  and  $\mathcal{L}_2 = [s_1, s_2]$ . We compute  $\text{bFV}(S_2)$  by computing the endpoints of  $\gamma(s_1, s_2)$ . In the  $i$ -th iteration with  $i \geq 3$ , we compute  $\text{bFV}(S_i)$  and maintain  $\mathcal{L}_i$  as follows. Let  $s_l$  and  $s_r$  be the first element and the last element in  $\mathcal{L}_{i-1}$ , respectively. Then there is a point  $p$  shared by  $\beta_{i-1}(s_l)$  and  $\beta_{i-1}(s_r)$ . By Lemma 8,  $s_i$  is valid if and only if  $p \in \beta_i(s_i)$ . If  $d(s_i, p) < d(s_l, p)$ ,  $s_i$  is not valid for  $FV(S_i)$ , and thus it is not valid for  $FV(S)$ . We set  $\mathcal{L}_i = \mathcal{L}_{i-1}$  and move on to the next iteration. If  $d(s_i, p) \geq d(s_l, p)$ ,  $s_i$  is valid for  $FV(S_i)$ . We set  $\mathcal{L}_i = \mathcal{L}_{i-1}$ . Then we update  $\text{bFV}(S_i)$  from  $\text{bFV}(S_{i-1})$  by computing the endpoints of  $\beta_i(s_i)$ . This can be done by searching them along the boundary of  $\Omega$  from  $p$ , once in clockwise orientation and once in counterclockwise orientation. In doing so, we update  $\mathcal{L}_i$  accordingly, and then append  $s_i$  to  $\mathcal{L}_i$ .

Consider the case that we search for an endpoint of  $\beta_i(s_i)$  along the boundary of  $\Omega$  in counterclockwise orientation from  $p$ . Let  $q$  be the endpoint of  $\beta_{i-1}(s_r)$  other than  $p$ . Observe that  $q \in \beta_{i-1}(s_{r'})$  for site  $s_{r'}$  previous to  $s_r$  in  $\mathcal{L}_{i-1}$ . If  $d(s_i, q) < d(s_{r'}, q)$ , one endpoint of

$\beta_i(s_i)$  lies on  $\beta_{i-1}(s_r)$ . We compute the endpoint of  $\gamma(s_r, s_i)$  on  $\beta_{i-1}(s_r)$ . Otherwise,  $s_r$  is not valid for  $\text{FV}(S_i)$ , and thus it is not valid for  $\text{FV}(S)$ . We remove  $s_r$  from  $\mathcal{L}_i$  and move on to  $s_{r'}$ . We repeat this until one endpoint of  $\beta_i(s_i)$  is found. See Figure 5.



■ **Figure 5** (a) In the  $i$ -th iteration,  $s_i$  is inserted. (b) If  $d(s_i, p) \geq d(s_l, p)$ ,  $s_i$  is valid for  $\text{FV}(S_i)$ . We compute the endpoints of  $\beta_{i-1}(s_i)$  along  $\partial\Omega$  from  $p$  in both orientations. (c)  $\text{bFV}(S_i)$ .

We find the other endpoint of  $\beta_i(s_i)$  in clockwise orientation similarly. After computing both endpoints of  $\beta_i(s_i)$ , we append  $s_i$  to  $\mathcal{L}_i$ .

► **Lemma 13** (Lemma 7 of [14]). *Given an  $m$ -sided convex polygon  $\Omega$  and any two points  $p, q \in \text{int}(\Omega)$ , the endpoints of  $\gamma(p, q)$  on  $\partial\Omega$  can be computed in  $O(\log^2 m)$  time.*

We can compute  $d(s_i, p)$  and  $d(s_l, p)$  in  $O(\log m)$  time. If  $d(s_i, p) < d(s_l, p)$ , we are done. If  $d(s_i, p) \geq d(s_l, p)$ , we identify all sites not valid for  $\text{FV}(S_i)$  among sites valid for  $\text{FV}(S_{i-1})$ , and remove them from  $\mathcal{L}_i$ . This takes  $O(n \log m)$  time in total over all insertion steps. Then we compute the endpoints of  $\beta_i(s_i)$ . Observe that one endpoint of  $\beta_i(s_i)$  is an endpoint of  $\gamma(s_i, s)$  and the other endpoint of  $\beta_i(s_i)$  is an endpoint of  $\gamma(s_i, s')$ , where  $s$  and  $s'$  are the first and the last elements in  $\mathcal{L}_i$ . We can compute the endpoints of  $\beta_i(s_i)$  in  $O(\log^2 m)$  time by Lemma 13. Since the number of sites is  $n$ , it takes  $O(n \log^2 m)$  time in total to compute  $\text{bFV}(S)$ .

► **Lemma 14.**  *$\text{bFV}(S)$  can be computed in  $O(n(\log n + \log^2 m))$  time.*

## 5.2 Computing $\text{FV}(S)$

We have preprocessed  $\text{bFV}(S)$  of size  $O(m)$  and all  $O(\min\{m, n\})$  sites valid for  $\text{FV}(S)$  and  $\text{bFV}(S)$  by Lemma 14. We give an algorithm for computing  $\text{FV}(S)$  in  $O(\min\{m \log m, m \log n\})$  time by subdividing  $\Omega$  into Voronoi cells using  $\text{bFV}(S)$ . Our algorithm is based on a divide-and-conquer technique similar to the one by Shamos and Hoey [24] that computes the nearest-site Voronoi diagram in the plane under the Euclidean metric. But the merge step requires a novel algorithmic idea and an in-depth analysis to reduce the running time as each bisector is a piecewise conic curve consisting of  $O(m)$  segments.

Let  $\hat{S} = \langle s_0, \dots, s_{t-1} \rangle$  denote the sequence of sites valid for  $\text{FV}(S)$  such that  $s_0, \dots, s_{t-1}$  appear in clockwise orientation along  $\text{conv}(\hat{S})$ . Observe  $t = O(\min\{m, n\})$ . We use modulo  $t$  for the indices. For a site  $s \in \hat{S}$ , let  $R(s)$  denote the region in  $\Omega$  bounded by  $sp, sq, \beta(s)$ , where  $p$  and  $q$  are two endpoints of  $\beta(s)$ . By Lemma 6,  $V(s) \subseteq R(s)$ . Observe that every spoke of  $s$  intersecting  $R(s)$  intersects  $V(s)$ . Let  $n(s)$  denote the number of the spokes of  $s$  intersecting  $R(s)$ . The total number of  $n(s)$  for all  $s \in \hat{S}$  is  $O(m)$  by Lemma 9.

We compute  $\text{FV}(\hat{S})$ , which is the same as  $\text{FV}(S)$ . Roughly speaking, we partition a site sequence into two subsequences,  $S_L$  and  $S_R$ , of roughly equal size, and compute  $\text{FV}(S_L \cup S_R)$  by merging  $\text{FV}(S_L)$  and  $\text{FV}(S_R)$  along  $\gamma(S_L, S_R)$  recursively. The bisector  $\gamma(S_L, S_R)$  satisfies

the property that any point of  $\Omega$  lying on one side of  $\gamma(S_L, S_R)$  is farthest from some site in  $S_L$  and any point of  $\Omega$  lying on the other side of  $\gamma(S_L, S_R)$  is farthest from some site in  $S_R$ . Observe that  $\gamma(S_L, S_R)$  is connected in  $\Omega$  with two distinct points on  $\partial\Omega$ . If  $\gamma(S_L, S_R)$  was not connected or it had more than two points on  $\partial\Omega$ , it partitions  $\partial\Omega$  into four or more pieces, each belonging to either  $\text{bFV}(S_L)$  or  $\text{bFV}(S_R)$ . Then the cells of  $\text{bFV}(S_L)$  or  $\text{bFV}(S_R)$  are not consecutive along  $\partial\Omega$ , contradicting Lemma 8. Also,  $\gamma(S_L, S_R)$  has no closed loop since no Voronoi cell in the loop is incident to  $\partial\Omega$ .

Consider the  $k$ -th recursive step of the algorithm. Let  $S_L$  and  $S_R$  be two input sequences of sites in the step. We have  $\text{FV}(S_L)$  and  $\text{FV}(S_R)$ . For a site  $s \in S_L \cup S_R$ , let  $V_k(s)$  denote the cell of  $s$  in  $\text{FV}(S_L \cup S_R)$ , and let  $V_{k-1}(s)$  denote the cell of  $s$  in  $\text{FV}(S_L)$  for  $s \in S_L$  and the cell of  $s$  in  $\text{FV}(S_R)$  for  $s \in S_R$ . Let  $\beta_k(s) = V_k(s) \cap \partial\Omega$  and  $R_k(s) = R(s) \cap V_k(s)$ . Let  $R_{k-1}(S_L) = \bigcup_{s \in S_L} R_{k-1}(s)$  and  $R_{k-1}(S_R) = \bigcup_{s \in S_R} R_{k-1}(s)$ .

If three consecutive sites  $s_{i-1}, s_i, s_{i+1}$  are contained in  $S_L \cup S_R$  for some  $i$ ,  $\beta_k(s_i)$  and  $\beta(s_i)$  are the same. Thus,  $V_k(s_i) \subseteq R(s_i)$  by Lemma 6, implying that  $R_k(s_i)$  is  $V_k(s_i)$ .

► **Lemma 15.** *The followings hold.*

1.  $\gamma(S_L, S_R) \cap R_{k-1}(S_L) \cap R_{k-1}(S_R)$  is connected.
2.  $\gamma(S_L, S_R) \setminus (R_{k-1}(S_L) \cap R_{k-1}(S_R))$  does not appear in  $\text{FV}(S)$ .
3.  $\gamma(S_L, S_R) \cap R_{k-1}(s)$  is connected for any  $s \in S_L \cup S_R$ .

**Proof.** Let  $\gamma = \gamma(S_L, S_R)$ . Consider Claim 1. Since  $\gamma$  has an endpoint in  $R_{k-1}(S_L) \cap R_{k-1}(S_R)$ , it suffices to show that  $\gamma \cap R_{k-1}(S_L)$  is connected and  $\gamma \cap R_{k-1}(S_R)$  is connected. Assume for the contradiction that  $\gamma \cap R_{k-1}(S_L)$  is not connected. Then there is a curve  $C$  contained in  $\gamma \setminus R_{k-1}(S_L)$  which has an endpoint on  $\partial R_{k-1}(s_i)$  for some site  $s_i \in S_L$ . Consider the case  $\{s_{i-1}, s_i, s_{i+1}\} \subseteq S_L \cup S_R$ . Then there is a point  $p \in \Omega \setminus R_{k-1}(s_i)$  such that the farthest site in  $S_L \cup S_R$  of  $p$  is  $s_i$ , contradicting  $V_k(s_i) \subseteq R_k(s_i) \subseteq R_{k-1}(s_i)$ .

Thus,  $s_{i-1} \notin S_L \cup S_R$  or  $s_{i+1} \notin S_L \cup S_R$ . By definition,  $\partial R_{k-1}(s_i)$  consists of a line segment  $\ell$  and a part of  $\gamma(s_i, s_l)$ 's for some  $s_l \in S_L$ . If  $C$  has an endpoint on  $\gamma(s_i, s_l)$ , there is a point  $p \in \Omega \setminus R_{k-1}(S_L)$  such that the farthest site of  $p$  is  $s_l$ . This contradicts  $p \in R_k(s_l) \subseteq R_{k-1}(s_l)$ . Thus,  $\gamma$  intersects  $\ell$  at least three times, contradicting Lemma 6. Therefore,  $\gamma \cap R_{k-1}(S_L)$  is connected. We can show that  $\gamma \cap R_{k-1}(S_R)$  is connected by exchanging the roles of  $S_L$  and  $S_R$ . Thus, Claim 1 holds.

Consider Claim 2. Let  $C$  be the part of  $\gamma(s_l, s_r)$  for  $s_l \in S_L$  and  $s_r \in S_R$  that appears in  $\text{FV}(S)$ . Then  $C \subseteq V(s_l) \subseteq V_k(s_l)$  and  $C \subseteq V(s_r) \subseteq V_k(s_r)$ . Since  $V(s) \subseteq R_{k-1}(s)$  for every  $s \in S_L \cup S_R$ ,  $C \subseteq R_{k-1}(s_l) \cap R_{k-1}(s_r)$ . Thus,  $C \subseteq R_{k-1}(S_L) \cap R_{k-1}(S_R)$ . By contraposition, Claim 2 holds.

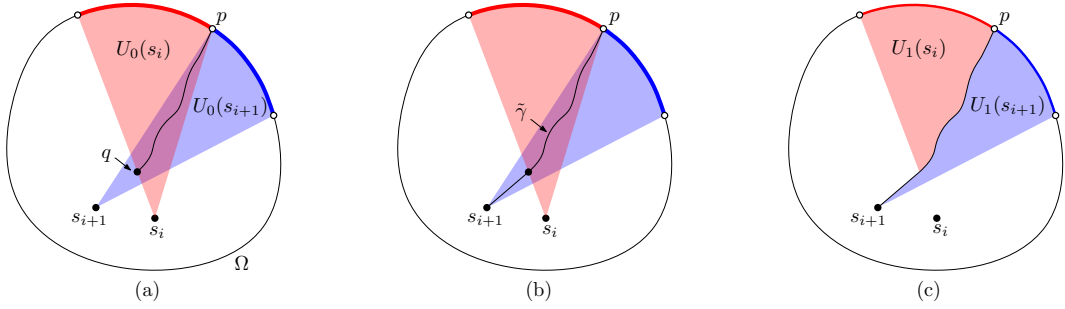
Consider Claim 3. Let  $s$  be a site in  $S_L$ . Let  $\tilde{\gamma}$  be the maximal portion of  $\gamma$  contained in  $R_{k-1}(S_L)$ . By Claim 1, it suffices to show that  $\tilde{\gamma} \cap R_{k-1}(s)$  is connected. Assume for the contradiction that  $\tilde{\gamma} \cap R_{k-1}(s)$  is not connected. Then there is a region  $R$  bounded by  $\tilde{\gamma}$  and  $R_{k-1}(s)$  satisfying  $R \not\subseteq R_{k-1}(s)$ . Since  $\tilde{\gamma}$  is connected,  $R$  does not intersect  $\partial\Omega$ . By Lemma 10, there is a site  $s' \in S_L \cup S_R$  with  $V_k(s') \subseteq R$ . This contradicts that each Voronoi cell intersects  $\partial\Omega$ . Similarly, we can show the case for  $s \in S_R$ . ◀

Lemma 15.1 guarantees that once we compute the endpoint of  $\gamma(S_L, S_R)$  contained in  $R_{k-1}(S_L) \cap R_{k-1}(S_R)$ , we can compute  $\gamma(S_L, S_R)$  within  $R_{k-1}(S_L) \cap R_{k-1}(S_R)$  by tracing the bisector from the endpoint. Also, Lemma 15.2 implies that it suffices to trace  $\gamma(S_L, S_R)$  within  $R_{k-1}(S_L) \cap R_{k-1}(S_R)$  in computing  $\text{FV}(S)$ .

### 5.2.1 Divide-and-conquer algorithm

Now we are ready to describe our algorithm for computing  $\text{FV}(\hat{S})$  from  $\text{bFV}(S)$ . In the  $k$ -th recursive step, we maintain a region  $U_k(s)$  which contains  $V_k(s)$  for  $s \in \hat{S}$ . As the base case, we initialize  $U_0(s)$  to  $R(s)$ . For the  $k$ -th recursive step, we compute  $U_k(s)$  from  $U_{k-1}(s)$  for  $k \geq 1$  inductively. In the last recursive step, we have  $U_k(s) = V(s)$  for every  $s \in \hat{S}$ .

Consider the recursive step with  $S_L = \langle s_i \rangle$  and  $S_R = \langle s_{i+1} \rangle$ . We compute the point  $p \in \beta(s_i) \cap \beta(s_{i+1})$ . Then we trace  $\gamma(s_i, s_{i+1})$  starting from  $p$  until the bisector meets  $\partial U_0(s_i)$  or  $\partial U_0(s_{i+1})$ . Consider the case that  $\gamma(s_i, s_{i+1})$  meets  $\partial U_0(s_i)$  at  $q$  first. We shoot a ray from  $q$  towards  $s_{i+1}$  and find the point  $r$  of  $\partial U_0(s_{i+1})$  hit by the ray. Let  $\tilde{\gamma}$  be the curve consisting of the part of  $\gamma(s_i, s_{i+1})$  from  $p$  to  $q$ , and  $qr$ . Then  $\tilde{\gamma}$  partitions  $U_0(s_i)$  and  $U_0(s_{i+1})$  into two subregions. We set  $U_1(s_j)$  to the subregion of  $U_0(s_j)$  containing  $\beta(s_j)$  for each  $j = i, i+1$ . See Figure 6. We handle the case that  $\gamma(s_i, s_{i+1})$  meets  $\partial U_0(s_{i+1})$  first analogously.



■ **Figure 6** (a) Tracing  $\gamma(s_i, s_{i+1})$  from  $p$ . (b) Ray from  $q$  towards  $s_{i+1}$ . (c)  $U_1(s_i)$  and  $U_1(s_{i+1})$ .

Consider the  $k$ -th recursive step. Let  $S_L$  and  $S_R$  be the two input sequences of sites. Without loss of generality, let  $s_i$  be the last site of  $S_L$  and  $s_{i+1}$  be the first site of  $S_R$ . Let  $U_{k-1}(S_L) = \bigcup_{s \in S_L} U_{k-1}(s)$  and  $U_{k-1}(S_R) = \bigcup_{s \in S_R} U_{k-1}(s)$ . We find the point  $p \in \beta(s_i) \cap \beta(s_{i+1})$ . Then we trace  $\gamma(s_i, s_{i+1})$  until it leaves (1)  $U_{k-1}(s_i)$ , (2)  $U_{k-1}(s_{i+1})$ , (3)  $U_{k-1}(S_L)$ , or (4)  $U_{k-1}(S_R)$ .

Consider the case that (1) holds but (3) does not hold. Let  $q$  be the point where  $\gamma(s_i, s_{i+1})$  leaves  $U_{k-1}(s_i)$  and  $\gamma(s_i, s_{i+1})$  enters  $U_{k-1}(s')$  for  $s' \in S_L$ . If  $U_{k-1}(s')$  has been visited before, we trace a ray from  $q$  towards  $s'' \in S_R$  satisfying  $q \in U_{k-1}(s'')$ , until the first intersection with  $\partial U_{k-1}(s'')$ . If  $U_{k-1}(s')$  has not been visited before, we repeat tracing  $\gamma(s_{i+1}, s')$  from  $q$  inwards  $U_{k-1}(s')$  as before until it leaves one of those four regions. See Figure 7(a). We handle the case that (2) holds but (4) does not hold analogously.

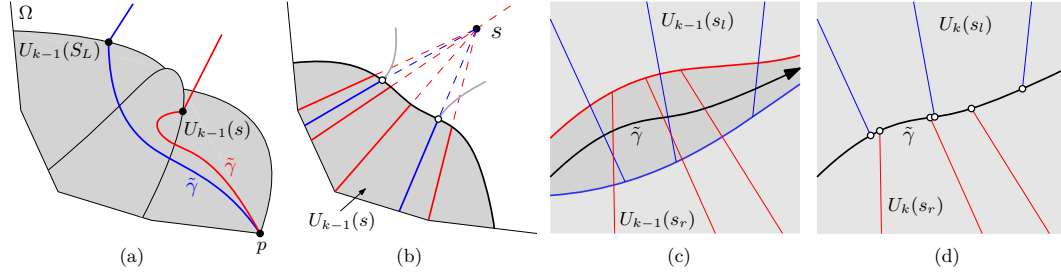
Consider the case that (3) holds. Let  $q$  be the point where  $\gamma(s_i, s_{i+1})$  leaves  $U_{k-1}(S_L)$ . We trace a ray from  $q$  towards  $s'' \in S_R$  satisfying  $q \in U_{k-1}(s'')$  until the first intersection point with  $\partial U_{k-1}(s'')$ . See Figure 7(a). We handle the case that (4) holds analogously.

Let  $\tilde{\gamma}$  be the resulting curve from the tracing above. Then  $\tilde{\gamma}$  partitions  $U_{k-1}(s)$  into two subregions for some  $s \in S_L \cup S_R$ . We set  $U_k(s)$  to the subregion of  $U_{k-1}(s)$  containing  $\beta(s)$ .

Observe that  $R_k(s) \subseteq U_k(s)$  for all  $s \in \hat{S}$  by the construction of the algorithm. Since  $p \in R_{k-1}(S_L) \cap R_{k-1}(S_R)$ , the following lemma holds.

► **Lemma 16.** *Let  $S_L$  and  $S_R$  be two input sequences in the  $k$ -th recursive step. Then  $\gamma(S_L, S_R)$  and  $\tilde{\gamma}$  are the same in  $R_{k-1}(S_L) \cap R_{k-1}(S_R)$ .*

We show how to maintain  $U_k(s)$  for all  $s \in \hat{S}$  in a map  $D_k(s)$ . Each region in  $D_k(s)$  has at most four sides. In the base case, we store the subdivision of  $U_0(s)$  by the spokes of  $s$  in  $\mathcal{D}_0(s)$  for each  $s \in \hat{S}$ . We construct  $\mathcal{D}_k(s)$  from  $\mathcal{D}_{k-1}(s)$  by shaving off the edges in  $\mathcal{D}_{k-1}(s)$



■ **Figure 7** (a)  $\tilde{\gamma}$  (blue) leaves  $U_{k-1}(S_L)$  or  $\tilde{\gamma}$  (red) visits  $U_{k-1}(s)$  twice. (b) Edges of type (1) (red), edges of type (2) (thick black), and edges of type (3) (blue). (c)  $U_{k-1}(s_l)$  and  $U_{k-1}(s_r)$  for  $s_l \in S_L$  and  $s_r \in S_R$ . Updating  $U_{k-1}(s_l)$  and  $U_{k-1}(s_r)$  along  $\tilde{\gamma}$ . (d)  $U_k(s_l)$  and  $U_k(s_r)$  after update.

along  $\tilde{\gamma}$  from an endpoint  $p \in \partial\Omega$ . Each edge of  $D_{k-1}(s)$  belongs to one of three types: (1) part of a spoke of  $s$ , (2) an edge connecting a Voronoi vertex and  $\beta(s)$ , and (3) part of  $\partial U_{k-1}(s) \setminus \beta(s)$ . See Figure 7(b). Observe that  $\tilde{\gamma} \cap U_{k-1}(s)$  is connected and it is part of the boundary of  $U_k(s)$ . When  $\tilde{\gamma}$  crosses an edge of type (1), we shave off the part of the edge not contained in  $U_k(s)$ . The resulting edge is incident to the intersection point. See Figure 7(c-d). Then we continue tracing  $\tilde{\gamma}$ . When  $\tilde{\gamma}$  crosses an edge of type (2), we remove the edge and continue tracing  $\tilde{\gamma}$ . When  $\tilde{\gamma}$  crosses an edge of type (3), we insert a Voronoi vertex  $v$  at the intersection and insert an edge  $\chi(s, v) \cap U_k(s)$  of type (3). If  $\tilde{\gamma}$  leaves  $D_{k-1}(s)$ , we finish the construction of  $D_k(s)$  by removing the boundary curve of  $D_{k-1}(s)$  from  $p$  to  $v$ .

### 5.2.2 Analysis

We analyze the running time for the  $k$ -th recursive step. Since we already have  $\text{bFV}(S)$ , we can find an endpoint of  $\gamma(S_L, S_R)$  in  $O(1)$  time. By Lemmas 15.3 and 16,  $\gamma(S_L, S_R)$  in  $U_{k-1}(S_L) \cap U_{k-1}(S_R)$  has complexity  $\sum_{s \in S_L \cup S_R} O(n(s))$ . Thus,  $\bigcup_{s \in S_L \cup S_R} U_{k-1}(s)$  has complexity  $\sum_{s \in S_L \cup S_R} O(n(s))$ . The same  $U_{k-1}(s)$  is visited  $O(1)$  times. We can check whether  $\gamma$  meets the same  $U_{k-1}(s)$  for the second time in  $O(1)$  additional time. The ray shooting and partitioning take time linear to the complexity of each cell.

Now we analyze the running time of the algorithm. The recursion depth is  $O(\log t) = O(\log \min\{m, n\})$  and  $\sum_{s \in S} n(s) = O(m)$  by Lemma 9. The total complexity of  $U_{k-1}(s)$  for sites  $s$  over all recursive calls at a fixed level  $k$  of recursion is  $O(m)$ . Thus, the algorithm runs in  $O(m \log \min\{m, n\})$  time, after computing  $\text{bFV}(S)$  in  $O(n \log n + n \log^2 m)$  time.

► **Theorem 17.** *The farthest-point Voronoi diagram of  $n$  point sites lying inside a convex  $m$ -gon in the Hilbert metric can be computed in  $O(n(\log n + \log^2 m) + m \log n)$  time.*

### References

- 1 Ahmed Abdelkader, Sunil Arya, Guilherme D. da Fonseca, and David M. Mount. Approximate nearest neighbor searching with non-Euclidean and weighted distances. In *Proceedings of the 13th Annual ACM-SIAM Symposium on Discrete Algorithms (SODA 2019)*, pages 355–372, 2019. URL: <https://dl.acm.org/doi/10.5555/3310435.3310458>.
- 2 Ahmed Abdelkader and David M. Mount. Economical Delone sets for approximating convex bodies. In *Proceedings of the 16th Scandinavian Symposium and Workshops on Algorithm Theory (SWAT 2018)*, volume 101, pages 4:1–4:12, 2018. doi:10.4230/LIPICS.SWAT.2018.4.
- 3 Ahmed Abdelkader and David M. Mount. Convex approximation and the Hilbert geometry. In *Proceedings of the 7th Symposium on Simplicity in Algorithms (SOSA 2024)*, pages 286–298, 2024. doi:10.1137/1.9781611977936.26.

- 4 Boris Aronov, Steven Fortune, and Gordon Wilfong. The furthest-site geodesic Voronoi diagram. *Discrete & Computational Geometry*, 9:217–255, 1993. doi:10.1007/BF02189321.
- 5 Rahul Arya, Sunil Arya, Guilherme D. da Fonseca, and David M. Mount. Optimal bound on the combinatorial complexity of approximating polytopes. *ACM Transactions on Algorithms*, 18(4):1–29, 2022. doi:10.1145/3559106.
- 6 Sunil Arya, Guilherme D. da Fonseca, and David M. Mount. Near-optimal  $\epsilon$ -kernel construction and related problems. In *Proceedings of 33rd International Symposium on Computational Geometry (SoCG 2017)*, volume 77, pages 10:1–10:15, 2017. doi:10.4230/LIPIcs.SocG.2017.10.
- 7 Sunil Arya, Guilherme D. da Fonseca, and David M. Mount. On the combinatorial complexity of approximating polytopes. *Discrete & Computational Geometry*, 58:849–870, 2017. doi:10.1007/S00454-016-9856-5.
- 8 Sunil Arya, Guilherme D. da Fonseca, and David M. Mount. Optimal approximate polytope membership. In *Proceedings of the 28th Annual ACM-SIAM Symposium on Discrete Algorithms (SODA 2017)*, pages 270–288, 2017.
- 9 Madeline Bumpus, Xufeng Caesar Dai, Auguste H. Gezalayan, Sam Munoz, Renita Santhoshkumar, Songyu Ye, and David M. Mount. Analysis of dynamic Voronoi diagrams in the Hilbert metric, 2024. arXiv:2304.02745.
- 10 L. Paul Chew and Robert L. Dyrsdale III. Voronoi diagrams based on convex distance functions. In *Proceedings of the 1st Annual Symposium on Computational geometry (SoCG 1985)*, pages 235–244, 1985.
- 11 Mark De Berg, Otfried Cheong, Marc Kreveld, and Mark Overmars. *Computational Geometry: Algorithms and Applications*. Springer Berlin, Heidelberg, 3rd edition, 2008.
- 12 Friedrich Eisenbrand, Nicolai Hähnle, and Martin Niemeier. Covering cubes and the closest vector problem. In *Proceedings of the 27th Annual Symposium on Computational geometry (SoCG 2011)*, pages 417–423, 2011. doi:10.1145/1998196.1998264.
- 13 Friedrich Eisenbrand and Moritz Venzin. Approximate CVP<sub>p</sub> in time  $2^{0.802n}$ . *Journal of Computer and System Sciences*, 124:129–139, 2022. doi:10.1016/J.JCSS.2021.09.006.
- 14 Auguste H. Gezalayan, Soo H. Kim, Carlos Lopez, Daniel Skora, Zofia Stefankovic, and David M. Mount. Delaunay triangulations in the Hilbert metric. In *Proceedings of the 19th Scandinavian Symposium and Workshops on Algorithm Theory (SWAT 2024)*, volume 294, pages 25:1–25:17, 2024. doi:10.4230/LIPICS.SWAT.2024.25.
- 15 Auguste H. Gezalayan and David M. Mount. Voronoi diagrams in the Hilbert metric. In *Proceedings of the 39th International Symposium on Computational Geometry (SoCG 2023)*, volume 258, pages 35:1–35:16, 2023. doi:10.4230/LIPICS.SocG.2023.35.
- 16 David Hilbert. Ueber die gerade Linie als kürzeste Verbindung zweier Punkte. *Mathematische Annalen*, 46(1):91–96, 1895.
- 17 Rolf Klein. Abstract Voronoi diagrams and their applications. In *Proceedings of Computational Geometry and its Applications (CG 1988)*, pages 148–157, 1988. doi:10.1007/3-540-50335-8\_31.
- 18 Der-Tsai Lee. Two-dimensional Voronoi diagrams in the  $L_p$ -metric. *Journal of the ACM*, 27(4):604–618, 1980. doi:10.1145/322217.322219.
- 19 Márton Naszódi and Moritz Venzin. Covering convex bodies and the closest vector problem. *Discrete & Computational Geometry*, 67(4):1191–1210, 2022. doi:10.1007/S00454-022-00392-X.
- 20 Frank Nielsen and Laetitia Shao. On balls in a Hilbert polygonal geometry. In *Proceedings of the 33rd International Symposium on Computational Geometry (SoCG 2017)*, volume 77, pages 67:1–67:4, 2017. doi:10.4230/LIPIcs.SocG.2017.67.
- 21 Athanase Papadopoulos and Marc Troyanov. *Handbook of Hilbert geometry*. European Mathematical Society, 2014.
- 22 Evantha Papadopoulou and D. T. Lee. The  $L_\infty$  Voronoi diagram of segments and VLSI applications. *International Journal of Computational Geometry & Applications*, 11(05):503–528, 2001.

- 23 Thomas Rothvoss and Moritz Venzin. Approximate CVP in time  $2^{0.802n}$  – Now in any norm! In *Proceedings of the 23rd International Conference on Integer Programming and Combinatorial Optimization (IPCO 2022)*, pages 440–453, 2022.
- 24 Michael Ian Shamos and Dan Hoey. Closest-point problems. In *Proceedings of the 16th Annual Symposium on Foundations of Computer Science (FOCS 1975)*, pages 151–162. IEEE, 1975. doi:10.1109/SFCS.1975.8.